Published in final edited form as:
Cancer Res. 2010 November 15; 70(22): 9483–9493. doi:10.1158/0008-5472.CAN-09-3880.

Silencing of autocrine motility factor induces mesenchymal to epithelial transition and suppression of osteosarcoma pulmonary metastasis

Yasufumi Niinaka[1,2,3], **Kiyoshi Harada**[1], **Masahiro Fujimuro**[4], **Masamitsu Oda**[1], **Arayo Haga**[3,5], **Misa Hosoki**[2], **Narikazu Uzawa**[2], **Naoya Arai**[2,6], **Satoshi Yamaguchi**[2], **Masashi Yamashiro**[2], and **Avraham Raz**[3]

[1]Department of Oral and Maxillofacial Surgery, University of Yamanashi, Faculty of Medicine, Chuo.

[2]Maxillofacial Surgery, Tokyo Medical and Dental University, Faculty of Dentistry, Tokyo.

[3]Tumor Progression and Metastasis Program, Karmanos Cancer Institute, Wayne State University, School of Medicine, Detroit.

[4]Department of Molecular and Cellular Biology, University of Yamanashi.

[5]Department of Drug and Housing Hygiene, Gifu Prefectural research Institute for Health and Environmental Science, Kakamigahara, Gifu.

[6]Department of Oral and Maxillofacial Surgery, University of Toyama, School of Medicine, Toyama.

Abstract

Phosphoglucose isomerase (PGI) is a multifunctional enzyme that functions in glucose metabolism as a glycolytic enzyme catalyzing an interconversion between glucose and fructose inside the cell, while, PGI acts as cytokine outside the cell, with properties that include autocrine motility factor (AMF) regulating tumor cell motility. Overexpression of AMF/PGI induces epithelial to mesenchymal transition (EMT) with enhanced malignancy. Recent studies have revealed that silencing of AMF/PGI resulted in mesenchymal to epithelial transition (MET) of human lung fibrosarcoma cells and breast cancer cells with reduced malignancy. Here, we constructed a hammerhead ribozyme specific against GUC triplet at the position G390 in the human, mouse, and rat AMF/PGI mRNA sequence. Mesenchymal human osteosarcoma MG-63, H S-Os-1, and murine LM8 cells were stably transfected with the ribozyme specific for AMF/PGI. The stable transfectant cells showed effective down-regulation of AMF/PGI expression and subsequent abrogation of AMF/PGI secretion, which resulted in morphological change with reduced growth, motility, and invasion. Silencing of AMF/PGI induced MET, in which up-regulation of E-cadherin and cytokeratins as well as down-regulation of vimentin were noted. The MET guided by AMF/PGI gene silencing induced osteosarcoma MG-63 to terminally differentiate into mature osteoblasts. Furthermore, The MET completely suppressed tumor growth and pulmonary metastasis of LM8 cells in nude mice. Thus, acquisition of malignancy might be completed in part by up-regulation of AMF/PGI and waiver of malignancy might be also controlled by down-regulation of AMF/PGI.

Requests for reprints: Yasufumi Niinaka, Department of Oral and Maxillofacial Surgery, University of Yamanashi, Faculty of Medicine, 1110 Shimokato, Chuo, Yamanashi 409-3898, Japan. Phone: +81-55-273-1111; Fax: +81-55-273-8210; yninaka@yamanashi.ac.jp.

Disclosure of potential Conflicts of Interest
No potential conflicts of interest were disclosed.

Keywords

autocrine-paracrine signaling; cell adhesion; cell adhesion and extracellular matrix; cell motility and migration; inducible gene expression; Metastasis/metastasis genes/metastasis models

Introduction

Epithelial to mesenchymal transition (EMT) is an essential mechanism for development of malignant cells for invasion and metastasis (1). EMT is a well-documented phenomenon occurring during embryonic development and wound healing as well as tumorigenesis (2). EMT was defined as the process that produces a complete loss of epithelial traits by the former epithelial cells accompanied by the acquisition of mesenchymal characteristics *in vitro*; *i.e.*, loss of epithelial markers and gain of mesenchymal markers (3,4). Normally, epithelial cells are polarized and tightly connected to each other; on the contrary, mesenchymal cells do not establish stable intercellular contacts (3,4). During EMT, epithelial cells lose intercellular junctions causing dissociation from the original mass (5).

Several growth factors and cytokines such as transforming growth factor-β (TGF-β) are known to initiate EMT (6). In the center of E-cadherin repression, a zinc finger transcription factor Snail functions as a molecular organizer by down-modulating epithelial genes and up-modulating mesenchymal genes, which is activated by most pathways triggering EMT and is negatively regulated by glycogen synthase kinase-3β (GSK-3β) (7). TGF-β acts through serine/threonine kinase receptors to phosphorylate the cytoplasmic Smads that activate the Snail family. The serine/threonine integrin linked kinase (ILK) is a signaling protein stimulated by both integrins and growth factor receptors. Activated ILK can directly phosphorylate downstream target GSK-3β, so resulting in the inhibition of GSK-3β activity, which stimulates the Wnt-β-catenin pathway and up-regulates Snail, that in basal conditions is suppressed by active GSK-3β.

Phosphoglucose isomerase (PGI) is a housekeeping cytosolic enzyme of sugar metabolism that plays a key role in both glycolysis and gluconeogenesis pathways (8), extracellularly it behaves as a cytokine that includes autocrine motility factor (AMF). Partial amino acid sequencing of fragment peptides (9) and molecular cloning and sequencing of AMF have identified as PGI (10). AMF is originally identified as a major cell motility-stimulating factor associated with cancer development and progression (11). Independently, PGI was found to be a neuroleukin promoting growth of embryonic spinal and sensory neurons (12), maturation factor mediating differentiation of human myeloid leukemia cells (13). Aberrations of presence in the serum and urine is of prognostic value associated with cancer progression (14–16). Overexpression of AMF/PGI induced transformation and survival of NIH-3T3 fibroblast through EMT with enhanced malignancy (17). To the contrary, down-regulation of AMF/PGI sensitized fibrosarcoma cells to oxidative stress to cellular senescence (18) and resulted in mesencymal to epithelial transition (MET) with reduced malignancy (19,20).

Ribozymes are RNA molecules with highly specific intrinsic enzymatic cleavage activity against target RNA sequence, which can discriminate mutant sequences differing by a single base from their wild-type counterparts (21). After binding to the RNA substrate by base pair complementation, the ribozyme cleaves the target RNA irreversibly. A hammerhead ribozyme has been identified as the smallest ribozyme composed of approximately 30 nucleotides with a conserved catalytic domain in the single-stranded region and variable stem regions formed by base-pairing with basically any desired target sequences (22). The characteristic site-specific cleavage of a phosphodiester bond after uridine of the triplet

GUC sequence (23) provides a very valuable tool for gene therapy as well as experimental gene targeting. A gene therapy trial using anti-HIV ribozyme, the first randomized, double-blind, placebo-controlled, phase 2 autologous cell-delivered gene transfer clinical trial, was carried out and indicated that cell-delivered gene transfer to be safe and biologically active (24). Thus, a ribozyme might be the one of the most reliable tools for gene therapy, of which safety and feasibility of the approach were already proven.

In the present report, we constructed a hammerhead ribozyme specific against GUC triplet at the position G390 in the AMF/PGI mRNA conserved sequence for the gene targeting. Then, we introduced the ribozyme into human and murine osteosarcoma cells to knock-down the translation and secretion of AMF/PGI.

Materials and methods

Plasmid construction and transfection

The AMF-targeted hammerhead ribozyme RzG390 was designed from a comparison of AMF cDNA sequences as shown in Fig. 1. In addition, a control ribozyme mRz with a single base pair mutation (A to G exchange) was prepared. Each pair of complemental oligonucleotides were artificially synthesized (Operon, Tokyo, Japan), annealed together and ligated into the BamHI/EcoRI sites of pBK-CMV (Stratagene, La Jolla, CA). Osteosarcoma cells were transfected with 8 μg of pBK-CMV ligated with or without Rz390G or mRz using 20 μl of Lipofectamin 2000 (invitrogen) as recommended by manufacturer's protocols. Stable transfectants were selected by 800 μg/ml of G418 (Sigma, St. Louis, MO) for one week and maintained with 100 μg/ml of G418.

Cells and cell culture

The human osteosarcoma cell line MG-63 was obtained in 2007 from the cell bank Riken Bioresource Center (Tsukuba, Ibaraki, Japan: routinely authenticated by short tandem repeat profiling (25)), and frozen as original stocks in 2007. The human HS-Os-1 and metastatic murine osteosarcoma cell line LM8 (26) were obtained in February 2010 from the cell bank Riken Bioresource Center. A human oral squamous cell carcinoma (SCC) cell line HSC-3 was established in 1989 (27), authenticated by short tandem repeat profiling in 2005, and frozen as original stocks in 2005 at Maxillofacail Surgery, Tokyo Medical and Dental University (Tokyo, Japan). All cells were grown in Dulbecco's modified Eagle's medium (DMEM) (Sigma) containing 10% heat-inactivated fetal bovine serum (FBS) (Sigma). Cultures were maintained at 37°C in an air–5% CO_2 incubator at constant humidity. To ensure maximal reproducibility, cultures were grown for no longer than six passages after recovery from original frozen stocks and monitored to prevent mycoplasma contamination (10).

Antibodies and chemicals

The recombinant human AMF (rhAMF) was affinity-purified by anti-AMF antibody conjugated with sepharose-beads, and polyclonal antibodies including anti-rhAMF were prepared by immunization of rabbit (Takara Shuzo, Shiga, Japan) as described previously (10,28). Mouse monoclonal antibodies AE1/AE3 to the human cytokeratins (Dako, Glostrup, Denmark), mouse monoclonal antibody VIM-13.2 to the human vimentin (Sigma), mouse monoclonal antibody 4A2C7 to E-cadherin (Invitrogen, Camarillo, CA) were all purchased. The secondary antibodies: horseradish peroxidase (HRPO)-conjugated goat anti-rabbit IgG antibody and HRPO-conjugated goat anti-mouse IgG antibody were purchased from Sigma.

Preparation of cell lysate and conditioned medium

After the cells reached to their 70–80% confluence, the medium was removed. The cells were washed twice with PBS and lysed in 1 ml/100 mm dish of cell lysis buffer, 25 mM Tris-HCl pH 7.8, 150 mM NaCl, 10 mM EDTA, 1% Deoxycholate-Na, 1% Triton X-100, 1% Aprotinin, 1% Leupeptin, 0.1 mM PMSF for cell lysate, or incubated with 5 ml/100 mm dish of serum-free DMEM (SF-DMEM) for 48 h to obtain conditioned medium. Cell supernatants were concentrated upto 100-fold using Amicon Ultra (30 kDa cut-off; Millipore, Billerica, MA). Protein concentrations of each sample were determined using Bio-Rad protein assay reagent (Bio-Rad, Hercules, CA) (10).

SDS-PAGE and western blotting

Aliquots of the cell lysates (25 μg) and the conditioned media (25 μg) were separated by 7.5% SDS-PAGE and blotted onto PVDF-plus membranes (MSI, Westborough, MA, USA). The blots were blocked with 5% nonfat dry milk in PBS overnight, and incubated with polyclonal antibody (1/3000) or monoclonal antibodies (1/1000) for 1 h at room temperature, followed by appropriate secondary antibodies (1/2500) for 1 h at room temperature. The labeled bands were revealed by chemiluminescence using ECL Western blotting detection reagents (Amersham, Arlington Heights, IL) and exposed to Kodak X-Omat film. Density of each band was quantitated with NIH Image software (10).

Phagokinetic track assay and invasion assay

Random cell motility (chemokinetics) was measured by phagokinetic track assay as described previously (10,28). Briefly, 2.0×10^3 cells were seeded on coverslip coated with 1.0% bovine serum albumin (BSA) and colloidal gold particles. After 24 h of incubation phagokinetic tracks were visualized under a microscope, and area cleared by at least 25 locomoted cells was measured using NIH Image software (http://www.rsb.info.nih.gov/ij/). The *in vitro* invasion assay was done using Transwell cell culture chambers (Corning Costar No. 3422, Corning, Lowell, MA) separated by 8.0-μm pore filter precoated with Matrigel (Collaborative Biomedical Products, Bedford, MA) on the upper surface. The bottom chamber was filled with DMEM supplemented with 10% FBS and cell suspensions of 1×10^5 cells/well were added onto the upper chamber. After 15 h incubation at 37°C, the top side of the insert membrane was scrubbed with a cotton swab and the bottom side was fixed with methanol and stained with 1% hematoxylin and eosin. Viable cells were counted under a microscope. Each assay was done in triplicate.

MTT assay

For cell proliferation, an MTT assay was done using Vybrant MTT Cell Proliferation Assay Kit (invitrogen) according to the manufacturer's instructions. Briefly, 1×10^3 cells per well were plated on 96-well plates and cultured for different times indicated in 100 μl of culture medium. At the end of the assay time, 10 μl of 12 mM MTT was added to each well and then incubated at 37°C for 4 h. 100 μl of solubilizing solution (SDS-HCl) was added and mixed thoroughly using pipette. The microplate was incubated air 37°C for 4 h in a humidified chamber. Plates were read at 570 nm on a spectrophotometric plate reader with a reference wavelength at 650 nm.

RT-PCR analysis

RT-PCR analysis was done as described previously (10). Total RNA was extracted using Trizol reagent (invitrogen) according to the manufacturer's protocols. The cDNA was generated by using random hexamer primers and reverse transcriptase SuperScriptIII (invitrogen). For quantitative evaluation of the amplified product, PCR encompassing 20 to 35 cycles was preliminarily done to determine the most suitable amplifications for each

reaction. PCR consisted of appropriate cycles of denaturing at 93°C for 30 sec, annealing at 62°C for 30 sec and extension at 72°C for 60 sec with initial denaturation at 93°C for 5 min and final extension at 72°C for 10 min, was carried out using PC320 (Astek, Yokohama, Japan). PCR-amplified products were electrophoresed in 0.75% agarose (H14 agarose, Takara, Tokyo, Japan) and stained with ethidium bromide. The PCR product size and the sequence of oligonucleotide primers were as shown in Table 1.

Pulmonarty metastatic assay in vivo

LM8parental, LM8mRz, and LM8Rz cells were inoculated subcutaneously (1×10^6 cells per mouse) into the back space of eight female BALB/c −nu/nu mice at 6 weeks of age, respectively. The tumor size was measured every week, and tumor volume was calculated with the following formula: tumor volume (mm^3) = $0.5XY^2$ (X and Y being the longest and shortest diameters of the tumor, respectively). Five weeks later, the subcutaneous tumor and lungs were removed to make frozen specimens. The specimens were cut at their maximum dimensions and fixed with 4% paraformaldehyde in PBS and stained either by hematoxylin and eosin or antibody. The number of lung metastatic nodules was counted microscopcally, and the occupancy was also microscopically calculated by NIH image.

Statistical analysis

Data are expressed as mean F SD. Comparisons between the groups were determined using unpaired t test. $P < 0.05$ was considered statistically significant.

Results

Suppression of AMF/PGI expression in MG-63 cells by RzG390

According to the cDNA sequence of human AMF/PGI, there are 22 GUC triplet sites, which are the target accessible for ribozymes to cleave (21–24). As shown in Figure 1, comparison of human, mouse, and rat cDNA for AMF/PGI indicated a well-conserved sequence around the GUC triplet at G390. Here, a ribozyme specific against GUC at the position G390 was synthesized and constructed in pBK-CMV (RzG390). In addition, a control ribozyme with point mutation (mRz) was introduced. Similarly forward and reverse primers of AMF/PGI were designed in the conserved sequence to utilize for human and mouse (Table 1). Human osteosarcoma MG-63 cells with mesenchymal origin were transfected with RzG390, mRZ, or vector only (mock). The stable transfectants were established by G418 selection, finally six clones of each were obtained. To examine the efficiency for AMF/PGI silencing, we detected the level of mRNA by RT-PCR and the level of protein expression by Western blot (Figure 2A). The RT-PCR showed that the level of AMF/PGI mRNA was efficiently decreased in the ribozyme transfectants (Rz), compared with MG-63 parental cells and other controls. No significant difference could be observed among clones in each parental, mock, or mRz group. Moreover, Rz cells showed decreased expression of endogenous AMF/PGI at protein level by Western blot analysis. AMF/PGI mRNA expression in Rz was remarkably suppressed and AMF secretion was abrogated, however, half of intracellular AMF/PGI was retained at the protein level (Figure 2A).

Effect of AMF/PGI gene silencing on tumor cell behaviors

We further analysed whether the complete abrogation of AMF/PGI secretion influenced cell growth, motility, and invasion. As shown in Figure 2B cell growth of Rz was slightly inhibited without significance. However, phagokinetic track assay representing intrinsic chemokinesis in Rz was drastically reduced to 20% compared with its parental counterpart and controls. Therefore, we also carried out *in vitro* invasion assay to depict whether the complete abrogation of AMF/PGI secretion influenced cell invasion. As shown in Figure 2C

in vitro invasion assay, gene silencing of AMF/PGI also reduced invasiveness to less than 50% compared with parental and control cells. Thus, the depletion of extracellular AMF/PGI reduced intrinsic cell motility and invasion in an autocrine manner. The cells were plated and cultured, and morphologies were monitored during progression from sparse monolayer (Figure 2D upper panel) to confluency (Figure 2D lower panel). The parental MG-63 cells maintained their mesenchymal elongated spindle-shaped fibroblast-like morphology. In sharp contrast, the Rz cells underwent a significant morphologic transformation whereby, under sparse conditions, the cells acquired a round flattened shape without elongated shape (Figure 2D upper panel). On reaching confluence, the Rz cells acquired a paving stone-like appearance, which is typical to epithelial monolayer (Figure 2D lower panel). Furthermore, the Rz cells seemed to be tightly contacted and to be contact inhibited as opposed to the control cells that continued at confluence to pile up in a typical mesenchymal growth pattern (data not shown).

Silencing of AMF/PGI leads MET in osteosarcoma cells

It is known that growth factors and cytokines such as TGF-β, FGF, EGF, and TNF-α, can regulate EMT (1,2). The reduction of cell motility and morphological changes in Rz cells prompted us to examine whether they are associated with loss of mesenchymal and/or gain of epithelial markers. Thus, the expression of the intermediate filaments vimentin cytokeratin was tested by Western blot analysis. Reduction of vimentin expression and concomitant broad and strong signals of lower molecules of cytokeratins were observed in Rz cells (data not shown), however, we could not address which cytokeratins are expressed in Rz cells by Western blot. Therefore, we further analyzed the expression of cytokeratins, K1 to K8 as known as basic (Type II) and K 13 to K20 as known as low molecular acidic (Type I), utilizing RT-PCR. As shown in Figure 3A, mesenchymal markers N-cadherin, vimentin, integrin linked kinase ILK, and alpha smooth muscle actin (α-SMA) were all down-regulated. Contrary to the mesenchymal markers, an epithelial marker E-cadherin was up-regulated. Similarly, most cytokeratins were up-regulated in Rz cells except for K13, K14, and K15. Thus, we concluded that silencing of AMF/PGI lead MET in osteosarcoma MG-63 cells.

Silencing of AMF/PGI changes signal transduction to MET

We proceeded to examine the expression of molecules related to signal transduction. Snail, Slug, Twist1 and Twist2 are transcription repressors that have a key role in EMT both during development and tumor progression (1,2,4). Of note, E-cadherin repressor Snail leads to the loss of polarity and morphologic change by repressing E-cadherin (7). The Wnt/beta-catenin pathway participates in EMT by activating snail (7). Transformig growth factor-β (TGF-β) is well known to induce EMT, in which cooperation of TGF-β and other signaling pathways is required. TGF-β initiates receptor phosphorylation and activates Snail family (29). Activated snail induces down-regulation of E-cadherin, which is negatively regulated by GSK-3β (7). We, therefore, examined RT-PCR for EMT related molecules including these molecules. As shown in Figure 3B, Snail expression was down-regulated in Rz cells, while the expressions of Slug, ZEB-1/delta EF-1, and ZEB-2/SIP1 were not altered. Twist1 was not expressed in those cells, Twist2 was rather down-regulated in Rz cells. TGF-β1 was not expressed in those cells, while, TGF-β2 and TGF-β3 were down-regulated in Rz cells. Interestingly, the expression level of GSK-3β was not altered. Thus, results obtained by RT-PCR confirmed that gene silencing of AMF/PGI induced MET.

Silencing of AMF/PGI induces MG-63 cells to differentiate into osteoblasts

MG-63 has been reported to differentiate into osteoblast (29), and to express E-cadherin, which maintained the activity and mRNA levels of alkaline phosphatase and osteocalcin (OC) (30). We therefore, investigated the possibility for MG-63 cells to differentiate into

osteoblasts by RT-PCR. As shown in Figure 3B, silencing of AMF induced MG-63 cells to express OC and osteopontin (OP). To differentiate into osteoblast transcription factor runt-related transcription factor 2 Runx2 is essential (30), which induces to produce type I collagen, OC, OP, and other proteins to form bone tissue. Osterix is a transcription factor with zinc-finger inducing to produce OC inevitable for calcification. OC is a bone specific protein and is produced by mature osteoblast (31). In the process of osteoblast differentiation, Runx2 and Osterix and canonical Wnt signaling molecules inhibit mesenchymal stem cells from differentiating into chondrocytes and adipocytes (30). After the commitment to osteoblast lineage, Runx2 maintains the osteoblasts in an immature stage, and Runx2 must be suppressed for immature osteoblasts to become fully mature osteoblasts (31). As shown in Figure 3B, the expression of Osterix was up-regulated in Rz cells, although the Runx2 was slightly suppressed in the Rz390G cells compared with other lineage. Lack of Twist gene expression in OC and OP expressing cells strongly suggested maturation of osteoblasts (31). To date, 19 different Wnt genes are recognized in human (32,33). As shown in Figure 3B, Wnt2b, Wnt5a, and Wnt9a were down-regulated in Rz cells, on the other hand, Wnt3, Wnt9b, Wnt10b, Wnt11, and Wnt16 were up-regulated.

Silencing of AMF/PGI induces osteosarcoma cells to reduce malignancy through MET

These data showed that AMF/PGI gene silencing induced MET in osteosarcoma MG-63 cells. Therefore, we further introduced the ribozyme into the other osteosarcoma cell lines; *i.e.*, murine metastatic osteosarcoma LM8 and human osteosarcoma HS-Os-1. As shown in Figure 4A, the ribozyme down-regulated the expression of AMF/PGI, and abrogated the secretion of extracellular AMF, concomitant with down-regulation of vimentin and up-regulation of E-cadherin in those cells. The growth of both LM8 and HS-Os-1 was slightly inhibited as shown in Figure 4B. Random cell motility and *in vitro* invasion of both LM8 and HS-Os-1 were also significantly suppressed by silencing of AMF/PGI (Figure 4C and 4D). These data were very similar to the behaviors observed in MG-63 cells. Therefore, we further performed RT-PCR on HS-Os-1 cells to characterize. Silencing of AMF/PGI up-regulated E-cadherin and cytokeratins and down-regulated vimentin, ILK, and N-cadherin. OC, OP, Wnt10b, and Wnt11 were up-regulated, while Wnt2b and Wnt5a were commonly down-regulated (data not shown). So, we concluded that silencing of AMF/PGI might induce MET and osteoblast differentiation in osteosarcoma cells. Thus, these data also suggested that silencing of AMF might result in loss of malignancy in osteosarcoma cells. Therefore, we further carried out experiments using nude mice to investigate whether silencing of AMF/PGI influence tumor growth and pulmonary metastasis of LM8. The murine osteosarcoma LM8 cells, with high metastatic potential to the lung (26), were inoculated subcutaneously into the back space of eight female BALB/c–nu/nu mice at 6 weeks of age. The tumor size was measured every week. Five weeks later, the subcutaneous tumor and lungs were removed to make frozen specimens. Contrary to the LM8parental and LM8mRz cells, LM8Rz cells neither formed tumor mass subcutaneously nor metastasized to the lung as shown in Figure 5A and 5B, respectively.

Discussion

Over all gene silencing of AMF/PGI and the following abrogation of AMF/PGI secretion resulted in reduction of cell growth, motility, invasion and pulmonary metastasis. Intracellular enzymatic activity of intrinsic PGI is more essential for an individual cell to survive, which seems to be minimum requirement for the cell, than to secret AMF as an extracellular form of AMF/PGI. Because PGI is observed in all cells ubiquitously, while secretion of AMF is observed in only tumor cells or activated T cells (10). Secretion pathway of AMF is not classical because PGI lacks signal sequences. AMF/PGI is secreted extracellularly by phosphorylation at serine 185 by casein kinase II (CKII) (34).

Additionally, calcium dependent mechanism or calcium ionophores may be important for the AMF secretion, because calcium ionophores enhanced AMF secretion and EDTA inhibited AMF secretion (data not shown). Secreted AMF/PGI functions as a growth factor as well as a motility factor (35). As shown in Figure 2B and 4B, knock-down of AMF/PGI affected the growth of osteosarcoma cells, especially in murine metastatic osteosarcoma cells LM8 (Figure 5A). Knock-down of AMF/PGI also reduced intrinsic chemokinesis and *in vitro* invasion (Figure 2C,4C, and 4D). Funasaka *et al.* showed that knock-down of AMF/PGI expression in fibrosarcoma HT1080 cells using small interfering RNA (siRNA) reduced cell growth, motility and cell invasion. Moreover, knock-down of PGI/AMF inhibited anchorage-independent growth of tumor cells and completely suppressed growth of tumor xenograft in nude mice (18). Furthermore, gene silencing of AMF/PGI completely suppressed tumor growth and pulmonary metastasis in nude mice (Figure 5A and 5B). These accumulated data suggested that knock-down of AMF/PGI induced MET and that the MET resulted in loss of malignancy or waiver of malignancy, although it was suggested that cancer cells probably use this MET process during the later stages of metastasis (36,37). Ribozyme provided a very valuable tool for gene targeting for induction of MET, suggesting that gene therapy by manipulation of EMT/MET utilizing rybozyme targeting AMF/PGI might be efficient at least in this case.

N-cadherin, vimentin, ILK, and α-SMA were all down-regulated in MG-63Rz cells, and E-cadherin and cytokeratins were up-regulated (in Figure 3A). Thus, Silencing of AMF/PGI in osteosarcoma MG-63 cells resulted in MET. TGF-β is known to activate Snail through phosphorylation of Smads, and Snail is known to suppress E-cadherin expression (36). TGF-βs also signal ILK, MAPK and PI3K pathway, and activated ILK can directly phosphorylate downstream target GSK-3β to inactivate (7). MG-63 cells do not express TGF-β1 but TGF-β2 and TGF-β3 (Figure 3B). Silencing of AMF/PGI reduced the TGF-β2 and TGF-β3 production and secretion, resulting in down-regulation of Snail, which released from the basal stage of suppression of E-cadherin. In addition, GSK-3β, a negative regulator of Snail, was stably expressed in MG-63 cells, and the activity of GSK-3β was also free of inhibition, because of shortage of ILK and snail as shown in Figure 3. Funasaka, et al. showed that knock-down of AMF/PGI using siRNA induced MET in fibrosarcoma HT1080 cells, in which vimentin was down-regulated and cytokeratins were up-regulated (18–20). Similarly, knock-down of AMF/PGI using siRNA induced MET in breast cancer MDA-MB-231cells, in which E-cadherin and GSK-3β were up-regulated, meanwhile fibronectin, Snail, and β-catenin were down-regulated (20). These accumulated data strongly suggested that knock-down of AMF/PGI might release the curse of E-cadherin suppression through up-regulation of GSK-3β and down-regulation of TGF-β, Snail, and ILK.

Loss of malignancy in osteosarcoma cells may be involved in the process of differentiation as well as MET, because it is well known that differentiated cells are less malignant in general (37). Wnt signals are also known to induce EMT, which is also negatively regulated by GSK-3β (7). Knock-down of AMF/PGI in osteosarcoma cells MG-63 and HS-Os-1 cells commonly reduced expression of Wnt2b and Wnt5a. Among them, Wnt2b functions as the stem cell factor for neural or retinal progenitor cells during embryogenesis, and also for gastric cancer, esophageal cancer and skin basal cell carcinoma during carcinogenesis (38). Thus, Wnt2b might be involved in progression of cancer via EMT. Similarly up-regulation of Wnt5a expression concomitant with down-regulation of Wnt4 was observed in mesenchymal phenotype of squamous cell carcinoma (SCC). Moreover, EMT through overexpression of Snail in SCC resulted in up-regulation of Wnt5a and ZEB-1 (delta EF1) and down-regulation of Wnt4 (39). However, MET through knock-down of PGI/AMF failed to down-regulate ZEB-1 and to up-regulate Wnt4 (Figure 3B). Silencing of AMF/PGI induced osteosarcoma MG-63 cells to up-regulate Wnt10b and Wnt11 gene expression, which might be important in differentiation because up-regulation of Wnt10b reported to

increase bone mass via enhancing osteoblast differentiation (32), and Wnt11 signals through both canonical (beta-catenin) and non-canonical pathways and was up-regulated during osteoblast differentiation and fracture healing (40). Moreover, temporal and spatial expression of AMF/PGI was observed in bone and cartilage cells during postnatal development and fracture repair, in which immature osteocytes had further differentiated toward mature osteoblasts, and the expression of AMF/PGI was decreased markedly (41). Thus, silencing of AMF might be involved in loss of malignancy through differentiation via MET.

Acknowledgments

We specially thank Dr. Kaoru Aida for his technical support in The Third Department of Internal Medicine, University of Yamanashi. We specially thank Dr. Yoshio Nakano, Dr. Masatoshi Higuchi, Tomoyasu Kawasaki, Dr. Ryu-ichi Nakazawa, Dr. Chieko Yoshida, Dr. Akihiro Dohi, and Dr. Ayako Miura for clinical support in the Department of Oral and Maxillofacial Surgery. We specially thank Dr. Katsushi Mukawa for his technical support in The Animal Research Institute, University of Yamanashi. We specially thank V. Powell for her editing of the manuscript.

Grant Support

Grant-in-Aid Japan #18592167: YN, #20659312: KH, and #21791983: MO. Grant-in-Aid project in University of Yamanashi (YN). The Television Yamanashi Science Development Fund of UTY, Yamanashi, Japan (YN). NIH grant CA-51714 (AR).

References

1. Thiery JP, Sleeman JP. Complex networks orchestrate epithelial-mesenchymal transition. Nat Rev Mol Cell Biol. 2006; 7:131–142. [PubMed: 16493418]
2. Hay ED. An overview of epithelio-mesenchymal transformation. Acta Anat. 1995; 154:8–20. [PubMed: 8714286]
3. Greenburg G, Hay ED. Epithelia suspended in collagen gels can lose polarity and express characteristics of migrating mesenchymal cells. J Cell Biol. 1982; 95:333–339. [PubMed: 7142291]
4. Hay ED. The mesenchymal cell, its role in the embryo, and the remarkable signaling mechanisms that create it. Dev Dyn. 2005; 233:706–720. [PubMed: 15937929]
5. Bates RC, Mercurio AM. The epithelial-mesenchymal transition (EMT) and colorectal cancer progression. Cancer Biol Ther. 2005; 4:365–370. [PubMed: 15846061]
6. Guarino M. Epithelial-mesenchymal transition and tumor invasio. Int J Biochem Cell Biol. 2007; 39:2153–2160. [PubMed: 17825600]
7. Bachelder RE, Yoon SO, Franci C, de Herreros AG, Mercurio AM. Glycogen synthase kinase-3 is an endogenous inhibitor of Snail transcription: Implication for the epithelial-mesenchymal transition. J Cell Biol. 2005; 168:29–33. [PubMed: 15631989]
8. Faik P, Walker JI, Redmill AA, Morgan MJ. Mouse glucose-6-phosphate isomerase and neuroleukin have identical 3' sequences. Nature. 1988; 332:455–457. [PubMed: 3352745]
9. Watanabe H, Takehana K, Date M, Shinozaki T, Raz A. Tumor cell autocrine motility factor is the neuroleukin/phosphohexose isomerase polypeptide. Cancer Res. 1996; 56:2960–2963. [PubMed: 8674049]
10. Niinaka Y, Paku S, Haga A, Watanabe H, Raz A. Expression and secretion of neuroleukin/phosphohexose isomerase/maturation factor as autocrine motility factor by tumor cells. Cancer Res. 1998; 58:2667–2674. [PubMed: 9635595]
11. Liotta LA, Mandler R, Murano G, et al. Tumor cell autocrine motility factor. Proc Natl Acad Sci USA. 1986; 83:3302–3306. [PubMed: 3085086]
12. Gurney ME, Apatoff BR, Spear GT, et al. Neuroleukin: a lymphokine product of lectin-stimulated T cells. Science. 1986; 234:574–581. [PubMed: 3020690]
13. Xu W, Seiter K, Feldman E, Ahmed T, Chiao JW. The differentiation and maturation mediator for human myeloid leukemia cells shares homology with neuroleukin or phosphoglucose isomerase. Blood. 1996; 87:4502–4506. [PubMed: 8639816]

14. Gomm SA, Keevil BG, Thatcher N, Hasleton PS, Swindell RS. The value of tumour markers in lung cancer. Br J Cancer. 1988; 58:797–804. [PubMed: 2906254]
15. Baumann M, Kappl A, Lang T, Brand K, Siegfried W, Paterok E. The diagnostic validity of the serum tumor marker phosphohexose isomerase (PHI) in patients with gastrointestinal, kidney, and breast cancer. Cancer Invest. 1990; 8:351–356. [PubMed: 2207761]
16. Filella X, Molina R, Jo J, Mas E, Ballesta AM. Serum phosphohexose isomerase activities in patients with colorectal cancer. Tumour Biol. 1991; 12:360–367. [PubMed: 1798910]
17. Tsutsumi S, Hogan V, Nabi IR, Raz A. Overexpression of the autocrine motility factor/phosphoglucose isomerase induces transformation and survival of NIH-3T3 fibroblasts. Cancer Res. 2003; 63:242–249. [PubMed: 12517804]
18. Funasaka T, Hu H, Hogan V, Raz A. Down-regultion of phosphoglucose isomerase/autocrine motility factor expression sensitizes human fibrosarcoma cells to oxidative stress leading to cellular senescence. J Biol Chem. 2007; 282:36362–36369. [PubMed: 17925402]
19. Funasaka T, Hu H, Yanagawa T, Hogan V, Raz A. Down-regulation of phosphoglucose isomerase/autocrine motility factor results in mesenchymal-to-epithelial transition of human lung fibrosarcoma cells. Cancer Res. 2009; 67:4236–4243. [PubMed: 17483335]
20. Funasaka T, Hogan V, Raz A. Phosphoglucose isomerase/autocrine motility factor mediates epithelial and mesenchymal phenotype conversions in breast cancer. Cancer Res. 2009; 69:5349–5356. [PubMed: 19531650]
21. Cech TR. Self-splicing of group I introns. Annu Rev Biochem. 1990; 59:543–568. [PubMed: 2197983]
22. Haseloff J, Gerlach WL. Simple RNA enzymes with new and highly specific endoribonuclease activities. Nature. 1988; 334:585–591. [PubMed: 2457170]
23. Kawasaki H, Ohkawa J, Tanishige N, et al. Selection of the best target site for ribozyme-mediated cleavage within a fusion gene for adenovirus E1A-associated 300 kDa protein (p300) and luciferase. Nucleic Acids Res. 1996; 24:3010–3016. [PubMed: 8760887]
24. Mitsuyasu RT, Merigan TC, Carr A, et al. Phase 2 gene therapy trial of an anti-HIV rebozyme in autologous CD34+ cells. Nature Med. 2009; 15:285–289. [PubMed: 19219022]
25. Cabrera CM, Cobo F, Nierto A, et al. Identity test: detarmination of cell line cross-contamination. Cytotechnology. 2006; 51:45–50. [PubMed: 19002894]
26. Asai T, Ueda T, Itoh K, et al. Establishment and characterization of a murine osteosarcoma cell line (LM8) with high metastatic potential to the lung. Int J Cancer. 1998; 76:418–422. [PubMed: 9579581]
27. Momose F, Araida T, Negishi A, Ichijo H, Shioda S, Sasaki S. Variant sublines with different metastatic potentials selected in nude mice from human oral squamous cell carcinoma. J Oral Pathol Med. 1989; 18:391–395. [PubMed: 2585303]
28. Niinaka Y, Haga A, Negishi A, Yoshimasu H, Raz A, Amagasa T. Regulation of cell motility via high and low affinity autocrine motility factor (AMF) receptor in human oral squamous carcinoma cells. Oral Oncol. 2002; 38:49–55. [PubMed: 11755821]
29. Parreno J, Buckley-Herd G, de-Hemptinne I, Hart DA. Osteoblastic differentiation, contraction, and mRNA expression in stress-relaxed 3D collagen I gels. Mol Cell Biochem. 2008; 317:21–32. [PubMed: 18566755]
30. Haÿ E, Lemonnier J, Modrowski D, Lomri A, Lasmoles F, Marie PJ. N- and E-cadherin mediate early human calvaria osteoblast differentiation promoted by bone morphogenetic protein-2. J Cell Physiol. 2000; 183:117–128. [PubMed: 10699973]
31. Komori T. Regulation of bone development and maintenance by Runx2. Front Biosci. 2008; 13:898–903. [PubMed: 17981598]
32. Bennett CN, Ouyang H, Ma YL, et al. Wnt10b increases postnatal bone formation by enhancing osteoblast diffenentiation. J Boine Mier Res. 2007; 22:1924–1932.
33. Katoh M. WNT2B: comparative integromics and clinical applications (Review). Int J Mol Med. 2005; 16:1103–1108. [PubMed: 16273293]
34. Haga A, Niinaka Y, Raz A. Phosphohexose isomerase/autocrine motility factor/neurokeukin/maturation factor is a multifunctional phosphoprotein. Biochim Biophys Acta. 2000; 1489:235–244. [PubMed: 11004567]

35. Tsutsumi S, Yanagawa T, Shimura T, et al. Regulation of cell proliferation by autocrine motility factor/phosphoglucose isomerase signaling. J Cell Biol. 2003; 278:32165–732172.

36. Batlle E, Sancho E, Franci C, et al. The transcription factor snail is a repressor of E-cadherin gene expression in epithelial tumour cells. Nat Cell Biol. 2000; 2:84–89. [PubMed: 10655587]

37. Niinaka Y, Oida S, Ishisaki A, et al. Autocrine motility factor and its receptor expressions in oral squamous cell carcinoma (SCC) cells. Int J Oncol. 1996; 9:433–438. [PubMed: 21541531]

38. Pignatelli M, Ansari TW, Gunter P, et al. Loss of membranous E-cadherin expression in pancreatic cancer: correlation with lymph node metastasis, high grade, and advanced stage. J Pathol. 1994; 174:243–248. [PubMed: 7884585]

39. Taki M, Kamata N, Yokoyama K, Fujimoto R, Tsutsumi S, Nagayama M. Down-regulation of Wnt-4 and up-regulation of Wnt-5a expression by epithelial-mesenchymal transition in human squamous carcinoma cells. Cancer Sci. 2003; 94:593–597. [PubMed: 12841867]

40. Friedman MS, Oyserman SM, Hankenson KD. Wnt11 promotes osteoblast maturation and mineralization through R-spondin 2. J Biol Chem. 2009; 284:14117–14125. [PubMed: 19213727]

41. Zhi J, Sommerfeldt DW, Rubin CT, Hadjiargyrou M. Differential expression of neuroleukin in osseous tissue and its involvement in mineralization during osteoblast differentiation. J Bone Mineral Res. 2001; 16:1994–2004.

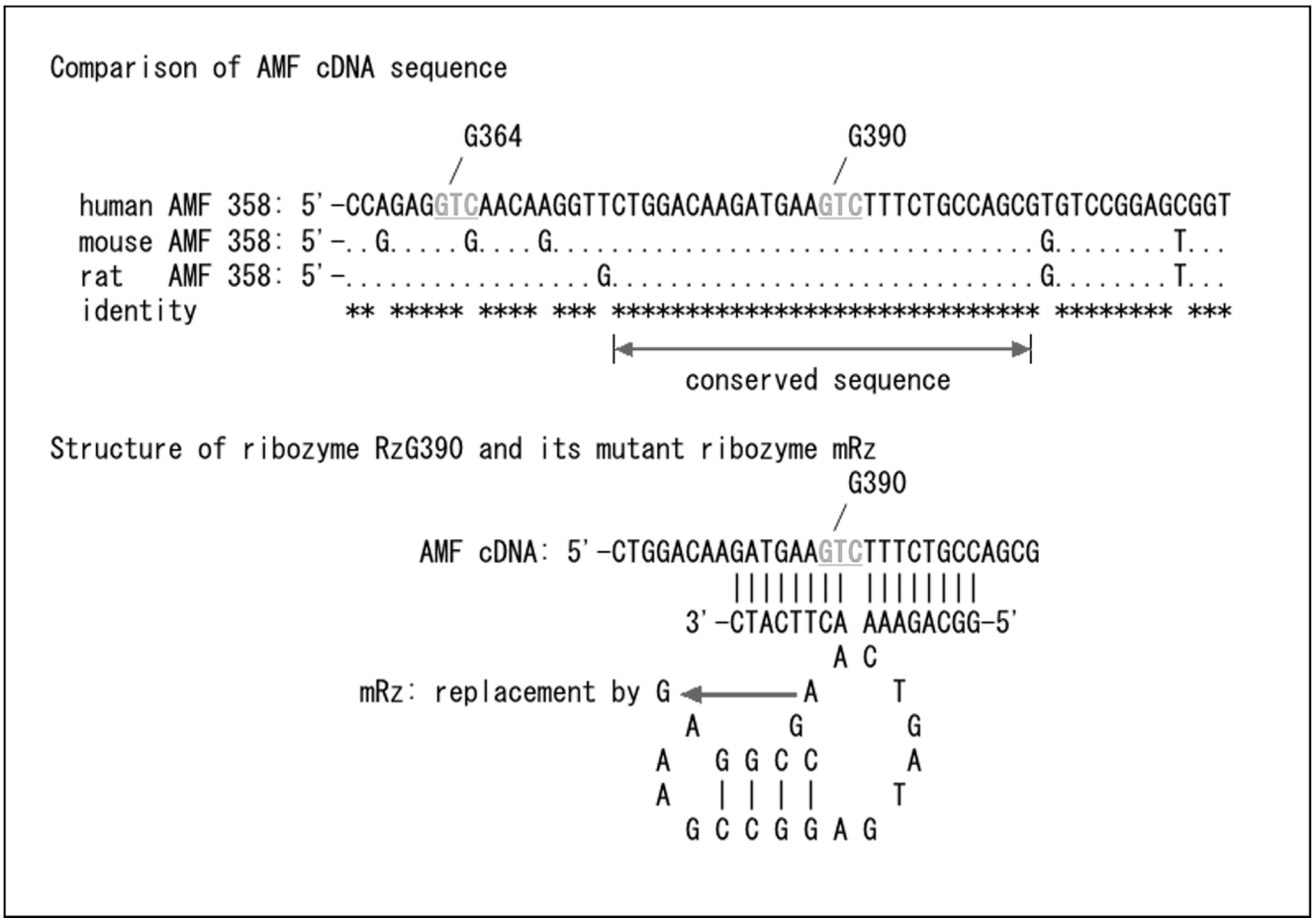

Figure 1.

Comparison of AMF cDNA sequences and structure of ribozyme. Identical nucleotides are indicated by aster (*) and putative GUC triplets are indicated in gray characters in a partial human cDNA sequence in comparison with mouse and rat. Structure of ribozyme consists of enzymatic core sequence, recognition sites, and restriction enzyme recognition arms. The sequence around G390 is well conserved and selected as a recognition sequence. A mutant ribozyme is also constructed by a single mutation with replacement of Adenine (A) by Guanine (G) in the enzymatic core sequence to lose catalytic activity.

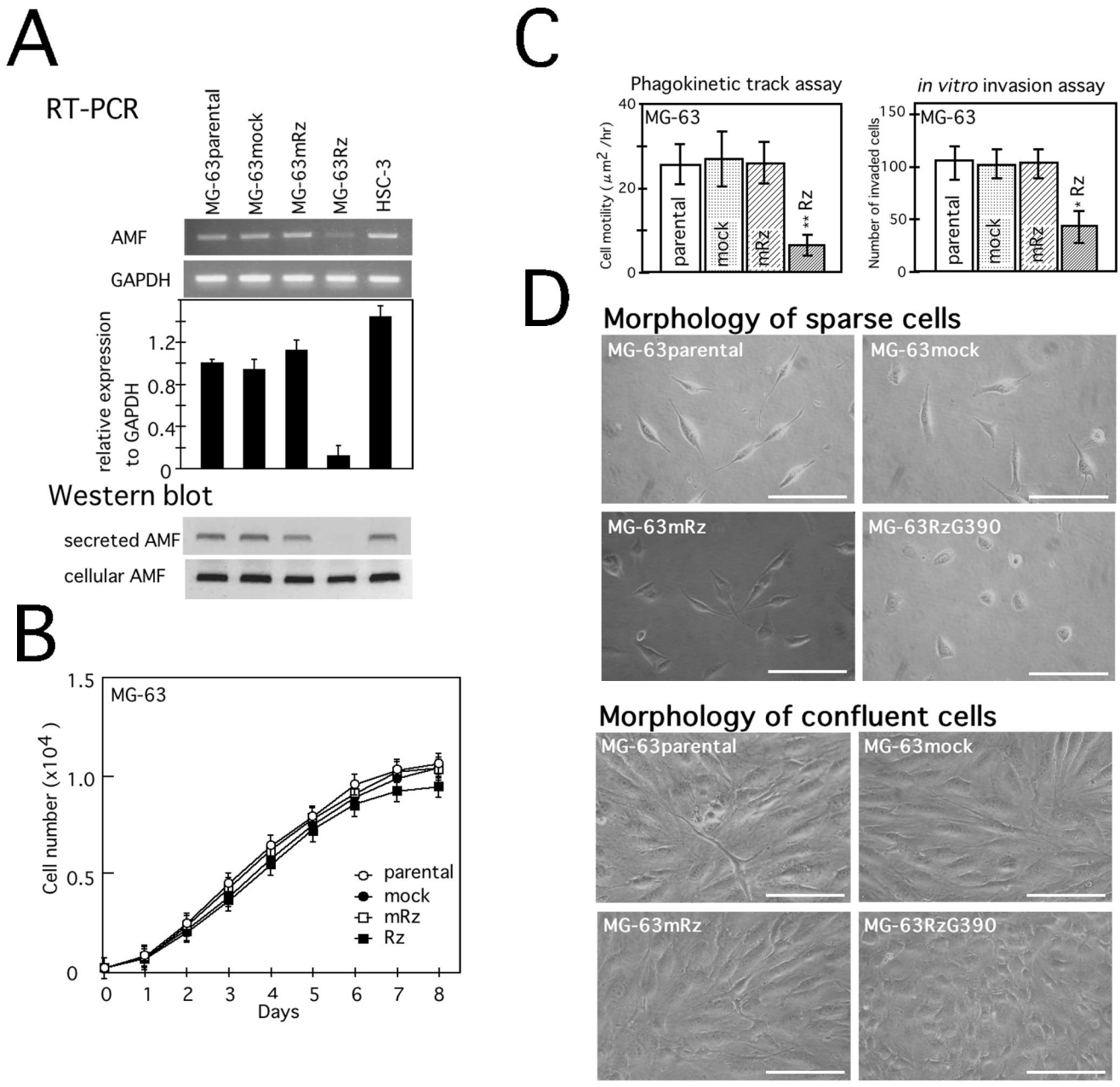

Figure 2.

Effect of AMF gene silencing in human osteosarcoma MG-63 cells (Rz) compared with parental, vector only transfected (mock), and mutant ribozyme transfected cells (mRz). A, Expression of AMF is evaluated by RT-PCR, and the relative expression to GAPDH is calculated. Extracellular secretion and intracellular expression of AMF are estimated by Western blot. B, Cell growth curve obtained by MTT assay. C, phagokinetic track assay and *in vitro* invasion assay, *, P<0.05; **, P<0.01, compared with control cells. D, Morphology of MG-63 cells cultured sparsely (upper panel) and densely (lower panel). Bur, 20 μm.

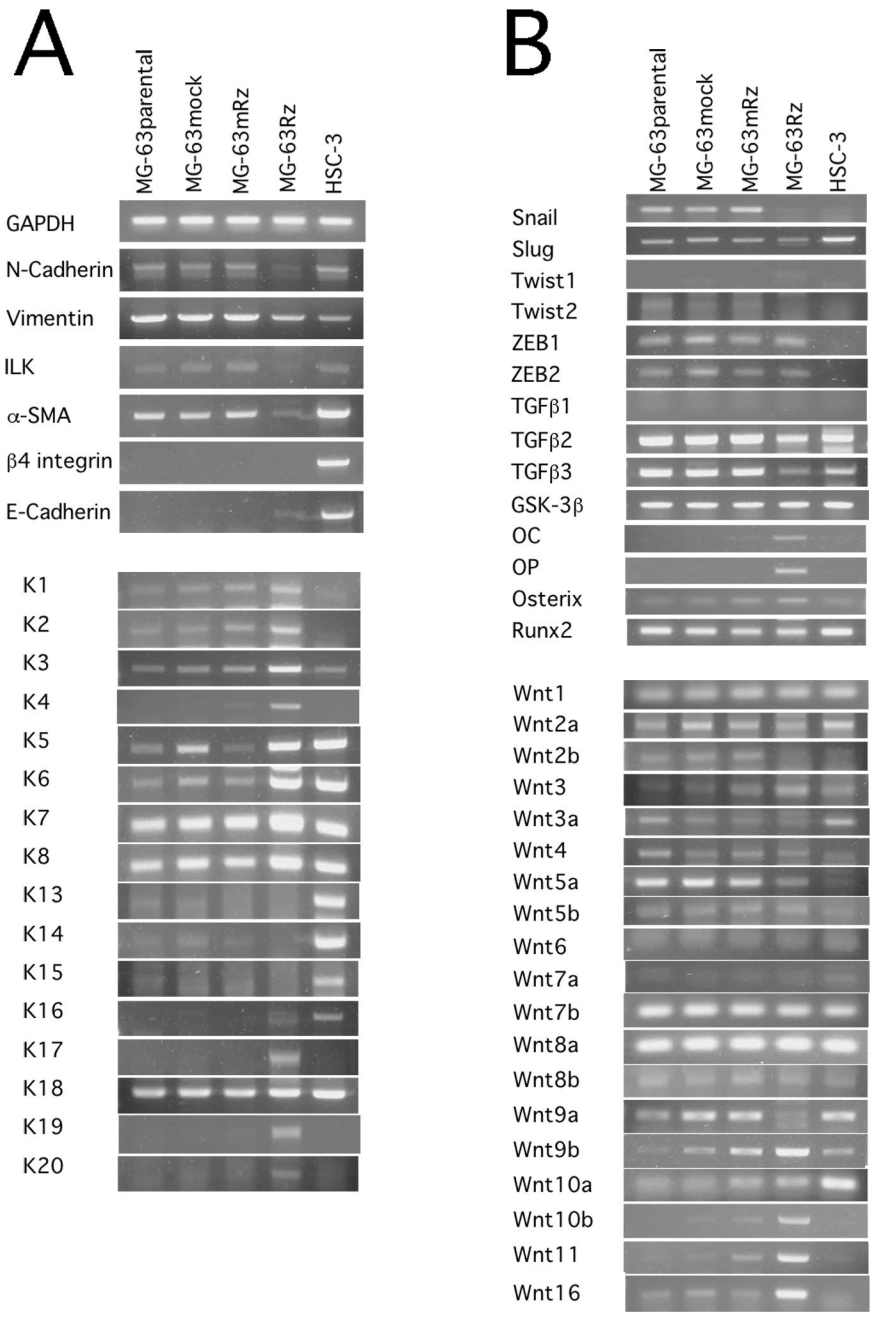

Figure 3.

RT-PCR. Silencing of AMF leads MET in osteosarcoma MG-63 cells. A, PCR for mesenchymal and epithelial markers. Mesenchymal markers: N-cadherin, Vimentin, ILK, and α-SMA, and epithelial markers: E-cadherin and cytokeratins (K1 to K8 as basic, and K13 to K20 as acidic). B, PCR for EMT related molecules, osteoblast differentiation related genes, and Wnt genes. Silencing of AMF induced MET in MG-63 cells and terminal differentiation into osteoblasts. B, Wnt2b, Wnt5a, and Wnt9a are suppressed, and Wnt3, Wnt10b, Wnt11, and Wnt16 are enhanced by AMF gene silencing.

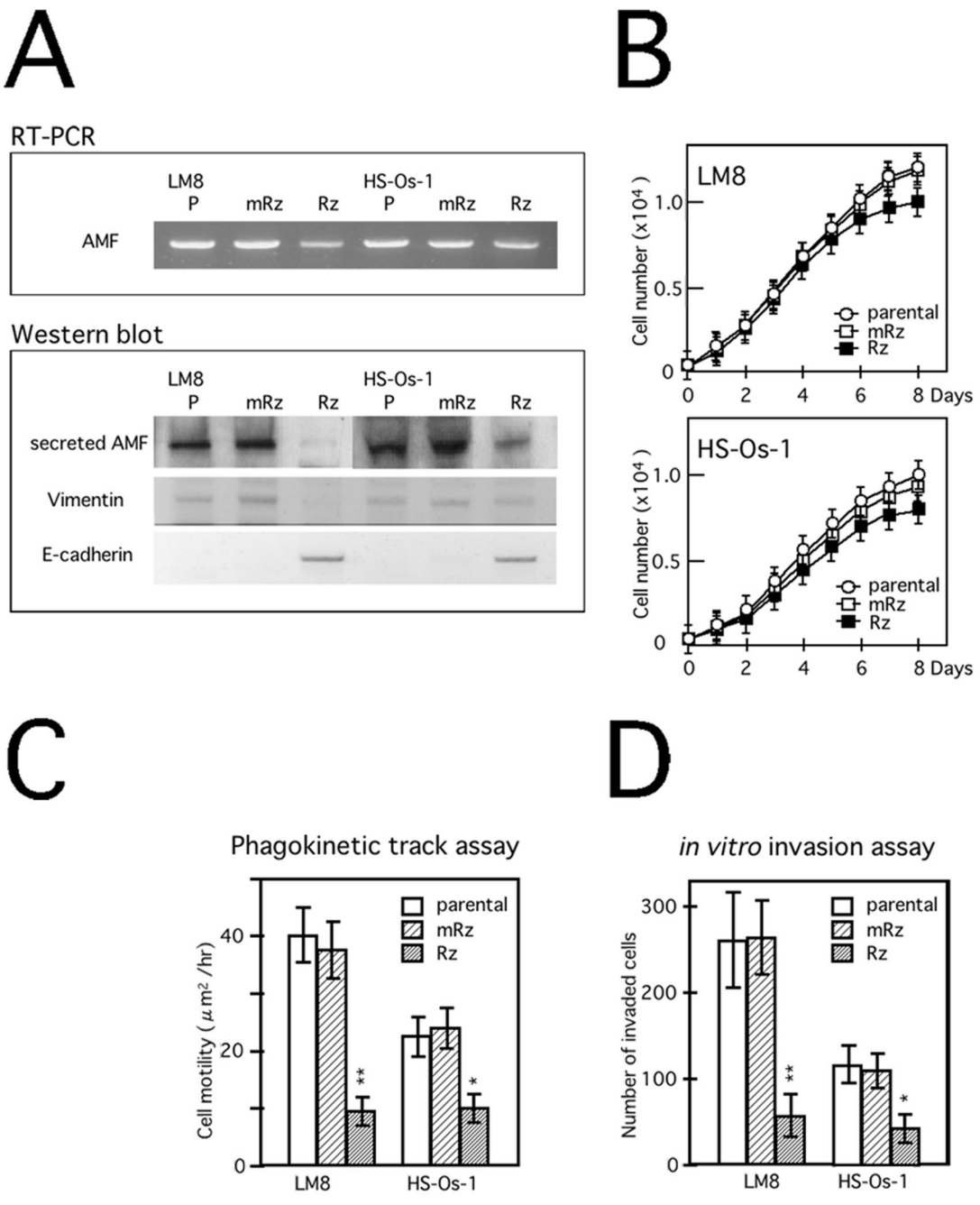

Figure 4.

Silencing of AMF in murine osteosarcoma LM8 and human HS-Os-1 cells. RzG390 treated (Rz) cells are compared with parental (P) and mutated ribozyme treated (mRz) cells. A, RT-PCR for expression of AMF and Western blot of secreted AMF and expression of vimentin and E-cadherin. Gene silencing of AMF induces MET in osteosarcoma cells. B, Cell growth curve obtained by MTT assay. C, phagokinetic track assay. D, *in vitro* invasion assay. *, P<0.05; **, P<0.01, Silencing of AMF induces LM8 and HS-Os-1 cells to reduce growth, motility, and *in vitro* invasion.

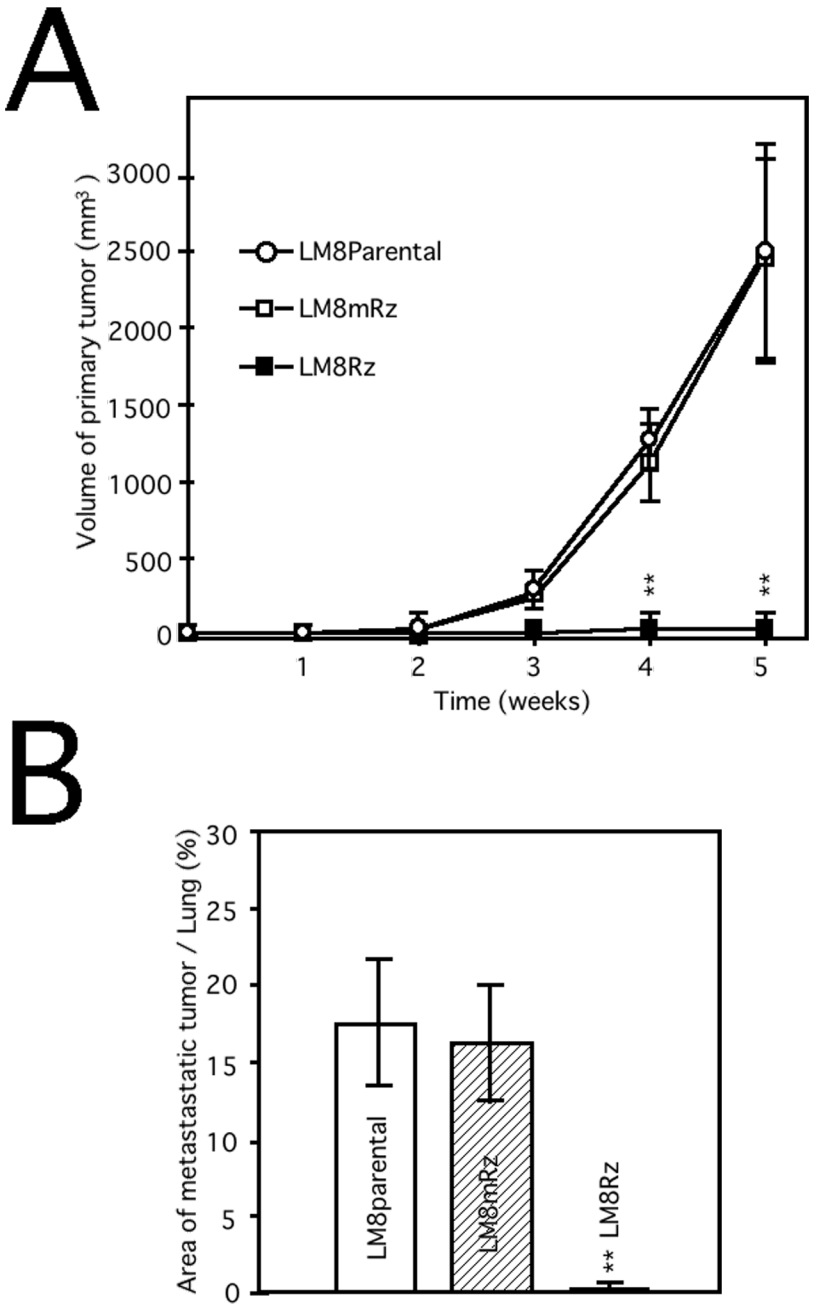

Figure 5.

Silencing of AMF/PGI suppresses tumor growth and pulmonary metastasis in nude mice, **, P<0.01. A, Dots represent tumor volume of primary site measured and calculated every week. Silencing of AMF suppresses tumor growth in nude mice. B, Columns represent the occupancy rate by tumor in the lung measured five weeks after inoculation. Silencing of AMF suppresses pulmonary metastasis in nude mice.

Table 1

List of PCR primers utilized in this study.

molecule	size(bp)	forward	reverse
AMF	1219	5'-GCTCCGCCATGGCCGCTCTC	5'-CACAGGGTATCATCTTGGTGCC
alpha-SMA	1148	5'-GTGCCAAGATGTGTGACGAC	5'-GGCATCTTAGAAGCATTTGCGG
E-cadherin	656	5'-GGCCAGCCATGGGCCCTTGG	5'-CACCTTCAGCCAACCTGTTT
GAPDH	206	5'-ACGACCACTTTGTCAAGCTC	5'-GGTCTACATGGCAACTGTGA
GSK-3beta	528	5'-GGCCACAAGAAGTCAGCTATACA	5'-CTGGTGCCCTATAGTACCGAGAA
ILK	1015	5'-AAGCTTGGGGTTCATCCTCCT	5'-TGTGTGTAGGAAGGCCATGC
integrin beta4	1156	5'-AGGGTGACTCCGAATCCGAA	5'-TTGGGGATGTTGAGCCGATG
K1	604	5'-TCTAAGTCAACATGAGTCGACAG	5'-ACCTTGTCAATGAAGGAGGCAA
K2	598	5'-ACAAAGGCATCATGAGTTGTCAG	5'-ACCTTGTCAATGAAGGAGGCAA
K3	658	5'-AGCTCCTTACCATGAGCAGACA	5'-ACCTTGTCAATGAAGGAGGCAA
K4	697	5'^GTGCCCTCCAGATGACTTCT	5'-ACCTTGTCGATGAAGGAGGCAA
K5	568	5'-AACAAGCCACCATGTCTGC	5'-ACCTTGTCGATGAAGGAGGCAA
K6	542	5'-CTCCTGGAACCATGGCCAGC	5'-ACCTTGTCGATGAAGGAGGCAA
K7	337	5'-GCCCAGCCACCATGTCCATC	5'-ACCTTGTCGATGAAGGAGGCAA
K8	337	5'-CTGCCTCTAACCATGTCCATC	5'-ACCTTGTCTATGAAGGAGGCAA
K13	510	5'-AAACAACCGGGTCATCCTGG	5'-TTCATGCTCAGCTGGGACTGCA
K14	440	5'-CAATGCCAATGTCCTTCTGC	5'-TTCATGCTGAGCTGGGACTGCA
K15	510	5'-CAACTCCCGGGTCATCCTGG	5'-TTCATGCTGAGCTGGGACTGCA
K16	999	5'-GCCAGTTCACCTCCTCCAGCTC	5'-ACTTCTTTGTTCAGCTCCTCGGT
K17	510	5'-CAATGCCAACATCCTGCTAC	5'-TTCATGCTGAGCTGGGACTGCA
K18	643	5'-TCCGCAAGGTCATTGATGACACC	5'-CTGCTGTCCAAGGCATCACCAA
K19	513	5'-GAACTCCAGGATTGTCCTGC	5'-TTCATGCTCAGCTGTGACTGCA
K20	581	5'-CACAAGCATCTGGGCAACACTG	5'-ATCCACTACTTCTTGCACGACTG
N-cadherin	900	5'-GAATCGTGTCTCAGGCTCCAAG	5'-GTAACACTTGAGGGGCATTGTC
Osteocalcin	264	5'-CTCACACTCCTCGCCCTATTGG	5'-CTCCTGAAAGCCGATGTGGTCAG
Osteopontin	341	5'-AGTCCAACGAAAGCCATGACCA	5'-GGTGATGTCCTCGTCTGTAGCAT
Osterix	316	5'-CTCTGCGGGACTCAACAACTCTG	5'-GAGCCATAGGGGTGTGTCATGTC
Runx2	298	5'-TGGACGAGGCAAGAGTTTCACCT	5'-CTGCCTGGGGTCTGTAATCTGAC
Slug	770	5'-CCTCCAAAAAGCCAAACTAC	5'-TCAGTGTGCTACACAGCAGC
Snail	320	5'-AATCGGAAGCCTAACTACAG	5'-GGAAGAGACTGAAGTAGAGG
TGF-beta1	335	5'-TGCTACCGCTGCTGTGGCTA	5'-TGCTGTTGTACAGGGCGAGC
TGF-beta2	510	5'-GAGAGGAGCGACGAAGAGTA	5'-CTGGTATATGTGGAGGTGCC
TGF-beta3	405	5'-ATGAAGATGCACTTGCAAAG	5'-CATTGAAGCGGAAAACCTTG
Twist1	664	5'-CTCGAGAGATGATGCAGGAC	5'-AATGACATCTAGGTCTCCGG
Twist2	451	5'-CGGGCGCCATGGAGGAGGGC	5'-CTAGTGGGACGCGGACATGG
Vimentin	675	5'-CTTCGCCAACTACATCGACA	5'-GCTTCAACGGCAAAGTTCTC
Wnt1	242	5'-CTACTTCGAGAAATCGCCCAAC	5'-ACAGACACTCGTGCAGTACGC
Wnt2	287	5'-GGGAATCTGCCTTTGTTTATGCCA	5'-GAACCGCTTTACAGCCTTCCTGC
Wnt2b	287	5'-CATCTCATCAGCAGGGGTAGTC	5'-GGCACTTACACTCCAGCTTCAG

molecule	size(bp)	forward	reverse
Wnt3	194	5'-CAGCAGTACACATCTCTGGGCTC	5'-CTGTCATCTATGGTGGTGCAGTTC
Wnt3a	330	5'-CTTTGTCCACGCCATTGCCTCAG	5'-ACCACCAGCATGTCTTCACCTCG
Wnt4	294	5'-CTGAAGGAGAAGTTTGATGGTGCC	5'-GTGGAATTTGCAGCTGCAGCGTTC
Wnt5a	273	5'-CTTCGCCCAGGTTGTAATTGAAGC	5'-CTGCCAAAAACAGAGGTGTTATCC
Wnt5b	304	5'-TGGGAGAGTCATGCAGATAGGC	5'-GGCCTCGTTGTTTTGCAGGTTC
Wnt6	300	5'-CTTGGTTATGGACCCTACCAGCAT	5'-CACTGCAGCAGCTCGCCCATAGA
Wnt7a	185	5'-AATGCCCGGACTCTCATGAACTG	5'-ACGGCCTCGTTGTACTTGTCCTTG
Wnt7b	196	5'-TCGGGAGATCAAGAAGAACGCG	5'-CGCGTTGTACTTCTCCTTCAGC
Wnt8a	511	5'-TCGAAAACTGTGGCTGTGATGGG	5'-CTGTTCTGTAGGCACTCACGACC
Wnt8b	315	5'-AGAGGCGATTTCCAAGCAGTTTG	5'-CGGGTAGAGATGGAGCGAAAGG
Wnt9a	453	5'-GCCAGTTCCAGTTCCGCTTTGAG	5'-TCAGATGCTTGCCCACCTCATG
Wnt9b	239	5'-CAACCTCAAGTACAGCACCAAGT	5'-AGTCATAGCGCAGTTTCAGCAC
Wnt10a	205	5'-CTGCACCGCTTACAACTGGATGC	5'-TTCTCGCGTGGATGTCTCTGTGA
Wnt10b	386	5'-ACTGTCCCGAGGCAAGAGTTTC	5'-AGGCTCCAGAATTGCGGTTGTG
Wnt11	365	5'-GACCTCAAGACCCGATACCTGT	5'-GGGCCTCACTTGCAGACATAGC
Wnt16	349	5'-CGGCTCCTGTGCTGTGAAAACAT	5'-CTTACACTCACACCTCTCCACGT
ZEB1 (deltaEF1)	436	5'-GTGGCCCATTACAGGCAACCAGT	5'-GCTAGGCTGCTCAAGACTGTAGT
ZEB2 (SIP1)	486	5'-AGTCCATGCGAACTGCCATCTGAT	5'-CTGGACCATCTACAGAGGCTTGTA